analytical chemistry

Technical Note

pubs.acs.org/ac

Integrating Optical Fiber Bridges in Microfluidic Devices to Create Multiple Excitation/Detection Points for Single Cell Analysis

Damith E. W. Patabadige,[†,§] Jalal Sadeghi,[†,‡,§] Madumali Kalubowilage,[†] Stefan H. Bossmann,[†] Anne H. Culbertson,[†] Hamid Latifi,[‡] and Christopher T. Culbertson*[,†]

[†]Department of Chemistry, Kansas State University, 1212 Mid-Campus Drive, Manhattan, Kansas 66506, United States

[‡]Laser and Plasma Research Institute, Shahid Beheshti University, Evin, Tehran, 1983963113, Iran

Supporting Information

ABSTRACT: A microfluidic device is reported that employs an out-of-plane optical fiber bridge to generate two excitation and two detection spots in a microfluidic channel using only one excitation source and one detector. This fiber optic bridge was integrated into a single cell analysis device to detect an intact cell just prior to lysis and the injected lysate 2, 5, 10, or 15 mm downstream of the injection point. Using this setup the absolute migration times for analytes from cells stochastically entering the lysis intersection could be determined for the first time in an automated fashion. This allowed the evaluation of several separation parameters, including analyte band velocity, migration time drift, diffusion coefficient, injection plug length, separation efficiency (N), and plate height (H), which previously could only be estimated. To demonstrate the utility of this system, a peptide substrate for protein kinase B (PKB) was designed, synthesized, and loaded into T-lymphocytes in order to measure PKB activity in individual cells. The optical fiber bridge is easy to implement, inexpensive, and flexible in terms of changing the distances between the two detection points.

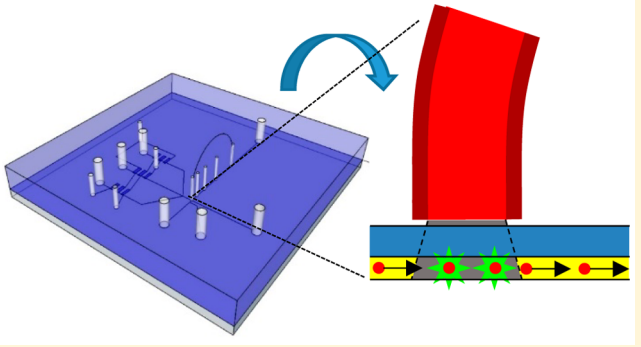

Because of the small footprint of microfluidic devices, the ability to integrate multiple optical detectors can be challenging.[1] In order to overcome this challenge the use of integrated optics have been reported[2] including on-chip waveguides fabricated by polymerization,[3,4] anisotropic silicon etching,[5,6] or ion-exchange.[7] These on-chip waveguides are, however, generally expensive, complex, and time-consuming to fabricate and often highly attenuate visible light in comparison to conventional optical fibers. In addition, such integrated optical waveguides are capable of transmitting light only between predetermined points.[8] An attractive alternative to the *in situ* fabrication of on-chip waveguides, therefore, is a system that employs optical fibers. Optical fibers have superior data transmission capability, have low light attenuation, are flexible, and are cost-effective.[9]

Previously, the integration of optical fibers has often been performed in the same plane as the microfluidic channel manifold and has been limited to static points along a microfluidic channel as the relative placements of the waveguides/fibers have not been tunable. Therefore, an off-chip integration approach using optical fibers potentially provides a better alternative since such fibers can be integrated at any point of interest without refabricating the microfluidic channel manifold. Such a fiber could be used as a bridge between two detection spots allowing the excitation and detection of fluorophores at any two given points in a microfluidic channel without significantly complicating the chip-fabrication process and the fluorescent detection system. For such a system, one end of the fiber would be placed above a detection point in a microfluidic channel specified by a focused laser from an external epi-illumination system (Figure 1). In addition to using the laser to excite analytes as they pass through the focused beam, this excitation light could be effectively coupled into the optical fiber and transmitted to a second excitation point. The ability of the fiber to transmit multiple wavelengths would allow the bridge then to collect the emission signal from the second detection point and transmit it back to first detection point where it would be collected by the epi-illumination system. Such a fiber bridge, therefore, would allow two excitation and detection points using only one excitation source and one detector thus considerably simplifying multiple point detection systems. In addition, the cost effectiveness of optical fibers (10 cm long optical fiber costs ~$0.30), the ease of integration compared to recently reported techniques,[10−12] and the compatibility with a wide range of wavelengths (250−1200 nm) would make such a system potentially interesting for a variety of microfluidic applications.

This fiber bridge could easily be used to improve single cell analysis on microfluidic platforms. Single cell manipulation in

Received: August 11, 2016
Accepted: September 14, 2016
Published: September 14, 2016

DOI: 10.1021/acs.analchem.6b03133
Anal. Chem. 2016, 88, 9920−9925

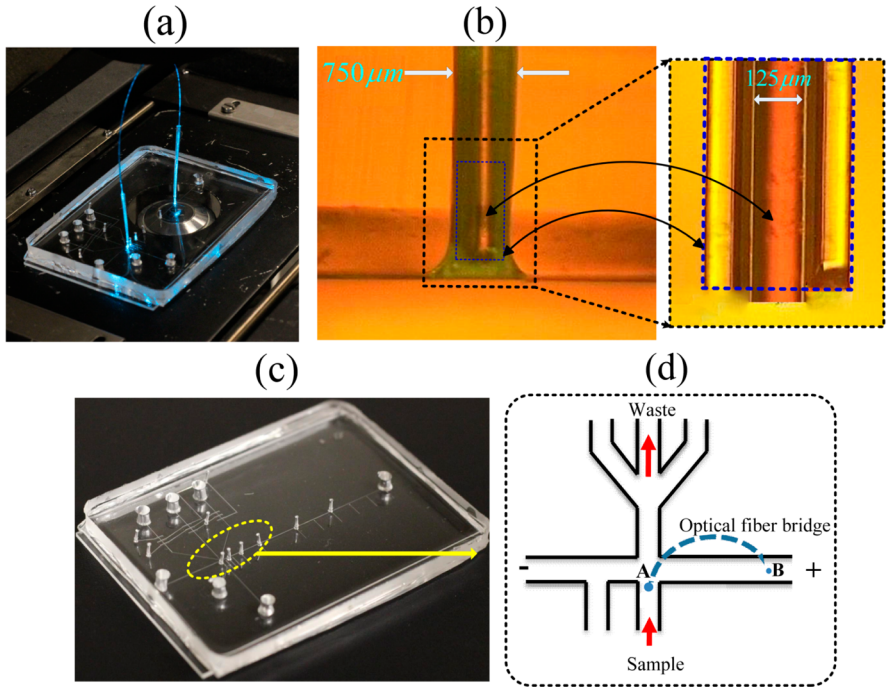

Figure 1. Overview of two-layer microfluidic device integrated with an optical fiber bridge: (a) a 20× objective was placed at LDP in order to transmit the excitation beam to the ZDP and collect the florescence from both the ZDP and LDP. The detection time difference between the two points is equivalent to the absolute migration time of the analyte of interest. (b) Cross section of ∼1 mm hole and a 20× micrograph of the fiber inserted through the plastic nozzle. The top layer of the device is ∼5 mm thick and the bottom-layer is 50 μm thick. The plastic nozzle restricts the free movement of the fiber. Vertical gap between the microfluidic channel and the fiber is 30 μm. 360° rotation of the nozzle and vertical movement of the fiber allows precise alignment in 3D space. (c and d) Photograph of the microfluidic device and expanded view of the cell lysing intersection. Points A and B are ZDP and LDP (any arbitrary point of interest downstream of the separation channel), respectively.

microfluidics typically consists of cell transport, cell lysis, and lysate injection followed by the electrophoretic separation of intracellular contents.[13−15] For detection in such systems, the excitation laser is generally focused through a microscopic objective and the fluorescent emission is collected through the same objective and sent to a detector. One major limitation of many current single cell separation systems that rely on the stochastic introduction of cells into the lysing intersection is that the actual lysing event is not detected as only one detector is employed in such systems and that detector detects the cell lysate. The reasons for this are generally 2-fold; first, there is little room to easily place two external excitation/detection systems at the lysis and lysate detection points as these two points are frequently only separated by a few millimeters. Second, there is significant extra expense in having an additional excitation source and detector. Being able to detect the lysis event, however, is important as it allows one to characterize how well a system is behaving, to monitor whether something begins to go wrong over the course of an analysis, and to identify analytes in a multicomponent separation based upon their absolute migration times. By being able to detect both the lysis event and the separated components of the cell lysate, several important separation parameters can be determined in an absolute way that cannot currently be accomplished using a single source and detector. These separation parameters include absolute migration time, migration time drift, peak variance, analyte dispersion, and the number theoretical plates generated (i.e., separation efficiency). The ability to understand such processes also allows the one to potentially improve separations. However, determining absolute migration times with microfluidic devices has rarely been reported.[16] One previous work demonstrated a fluorescence-based static imaging technique using a high resolution CCD camera.[16] The accuracy of these types of techniques depends on image quality. In addition, such approaches are restricted by the field of view of the camera to a limited distance downstream in the separation channel. If such limitations can be overcome using a fiber bridging technique, then more precise and accurate separation parameter measurements could be produced in real-time.

In addition to being able to monitor the how well a separation system is working, the ability to determine absolute migration times is very useful in the identification of analytes in a multicomponent separation especially if one or more of the components are expected to be missing in any given separation. For example, if one is measuring the activity of a kinase in a cell using a peptide specific substrate which was been loaded in that cell, the level of the activity of that kinase will determine whether either the phosphorylated or nonphosphorylated version of the peptide or both will be detected in the separation. Without the injection (or 0) time marker provided by the fiber optic bridge it would be impossible to tell the difference between a cell in which all or none of the substrate was phosphorylated.

In this paper, we introduce a microchip that uses an out-of-plane optical fiber bridge to connect optically 2 points along a fluidic channel. Single cells were driven toward the cell lysing intersection using multilayer soft lithographic valves, cells were lysed at the intersection in the presence of an external electric field applied across the separation channel, and the cell lysate was injected into the separation channel. The out-of-plane optical fiber bridge allowed the detection of both intact cells

DOI: 10.1021/acs.analchem.6b03133
Anal. Chem. 2016, 88, 9920−9925

just prior to lysis and the downstream lysate with a single laser excitation source and fluorescent detector. As a proof of principle, the separation characteristics of 6-carboxyfluorescein diacetate (6-CFDA) released from single cells were evaluated. Furthermore, a fluorescently tagged peptide substrate that can be used to monitor the activity of protein kinase B (PKB) was introduced into single cells.[17] These cells were lysed and the activity of the kinase qualitatively determined from the ratio of the phosphorylated and nonphosphorylated peptide peaks.

EXPERIMENTAL SECTION

Reagents and Materials. The reagents and materials are similar to that used previously.[18] A detailed list and sources can be found in the Supporting Information.

Fluorescent Peptide Synthesis. The rhodamine B (R_B) labeled myristoyl-based peptide substrate [R_B-GRPRAAT-FAEGC-s-s-C-K(Myr)-K-K-K-K (SPKB-Myr), where the amino acids are shown with standard notations and -s-s- represents disulfide linkage] was synthesized by means of solid-supported peptide synthesis.[19] Details of the synthesis are provided in the Supporting Information.

Cell Labeling. T-Lymphocytes (Jurkat cells) were obtained from ATCC (TIB-152 American Type Culture Collection, Rockville, MD) and cultured according to ATCC recommendations. The cells were labled with CFDA as previously described.[18] (see the Supporting Information for details). For the PKB single cell assay, the SPKB-Myr substrate was loaded into the cells in a manner similar to a previouly reported protocol.[20] (see the Supporting Information for more details).

Microchip Fabrication and Operation. A two-layer microfluidic device was fabricated using multilayer soft lithographic techniques and operated in a manner similar to previous reports.[18]

Detection. The 488 nm line from a multiline argon-ion laser (MellesGriot Laser Group, Carlsbad, CA) was used as the excitation source and directed into the rear port of a commercial inverted Nikon TS-100 microscope (Nikon Instruments, Inc., Melville, NY). The beam passed through a XF101-2 filter cube (Omega Optical) and was focused into the separation channel using a 20× objective (Plan Fluor, Nikon). A few centimeters of multimode silica optical fiber (Thorlabs FG105UCA, 105/125-μm multimode, N.A. = 0.22), which had been stripped of its protective polymeric coating, was bridged between the detection point and the injection intersection. As shown in Figure 1a,b, a plastic nozzle (i.e., pipet tip) segment (1 cm long) was used to hold the ends of the optical fiber in place on the microchip. Over the 1 cm length of the pipet, the cone diameter tapered from 1 mm down to 300 μm. Both ends of the fiber were cleaned, cleaved, and inserted into the pipet tips which were inserted into the holes on the microchip perpendicular to the channel. This method has the advantage that while fiber is fixed in the nozzle, the *X*, *Y*, and *Z* position of the fiber's cross section relative to the channels could be precisely adjusted and observed by moving the nozzle. Since the end of the fiber is in contact with the top of the bottom PDMS layer, the vertical gap (~32 μm) between the end of the fiber and the channel is equal to the thickness of the PDMS bottom layer (~50 μm) minus the molded channel depth (~18 μm). The focused excitation beam from the 20× microscope objective could be easily coupled into the bridged fiber at the lysate detection point (LDP, Figure 1a). The fiber then transmitted the excitation light to the lysis intersection (zero detection point; ZDP) where intact fluorescently labeled cells could be excited. The same fiber used for excitation was then used to collect the fluorescent emission from the intact, excited cells. After the cells were lysed, the lysate was injected and electrophoretically transported down the separation channel toward the anode. The focused beam from the microscope objective was used to excite the cell lysate and collect the fluorescent emission at the LDP. The fluorescence from both the intact cell and lysate was collected by the 20× microscope objective, passed through the XF101-2 filter cube, a 488.0 nm holographic notch filter (Kaiser Optical), and a 800 μm diameter pinhole before being detected by an R-928 photomultiplier tube (PMT, Hamamatsu Instruments, Bridgewater, NJ) attached to the trinolucular port of the microscope. The current from the PMT was amplified using a preamplifier at 50 μA/V with 100 Hz low-pass filter (Stanford Research Systems, Sunnyvale, CA) and sampled at 500 Hz using a PC1-6036E I/O card (National Instruments, Austin, TX). With this configuration both the intact cell and lysate were excited with one laser source and detected using one PMT.

RESULTS AND DISCUSSION

Transmission and Coupling Efficiency of the Bridged Fiber Configuration. The transmission and light coupling efficiencies of a 50 and a 105 μm diameter inner core optical fiber bridge were calculated theoretically and determined experimentally. As explained in the Supporting Information, the overall sensitivity of the 105 μm core fiber was significantly higher than for the 50 μm core fiber. The theoretical coupling efficiency for the 105 μm diameter multimodal fiber was calculated to be ~94% (please see the Supporting Information for details) while the actual coupling efficiency for the fiber was determined to be 45 ± 5% (please see the Supporting Information for details). Although the coupling efficiency was not 100%, it was constant for any given device. This, therefore, allowed not only the determination of absolute migration times but also created the potential to monitor the efficiency of cell lysate injection or the progress of chemical reactions via the relative intensity changes between the two detection spots.

Single Cell Analysis. For the results reported below, a 12 cm long 105/125 μm fiber was integrated between the zero detection point (i.e., the cell lysis intersection) and a point either 2 mm, 5 mm, 10 mm, or 15 mm downstream of the separation channel. Cells were transported to the lysis intersection at an average linear flow rate of 550 ± 23 μm/s. At this flow rate, ~100% of the lysate was injected into the separation channel while the cell debris was effectively removed from the lysis intersection by hydrodynamic flow toward the waste reservoirs.[18] As each cell passed the ZDP, a narrow peak was produced which represented the separation start time (t = 0). A second broadened peak was then detected a few seconds later which corresponded to the injection plug (Figure 2). The two peaks from each cell could easily be differentiated and correlated by eye based upon peak height, width, and relative separation distances between the peaks (Figure 3). However, we have developed and previously described an automated system for selecting correlated peaks based upon peak heights, areas, and relative separation distances that can be used in the future for the automated analysis of a large number of cells.[21] In rare cases where the electropherograms/peaks from 2 cells overlapped, the data were not analyzed. From these two peaks, the absolute migration time at a variety of separation distances was determined (Figure 3b, Table 1, and Figure S2). For a given separation distance, mean, median, and mode values were

DOI: 10.1021/acs.analchem.6b03133
Anal. Chem. 2016, 88, 9920−9925

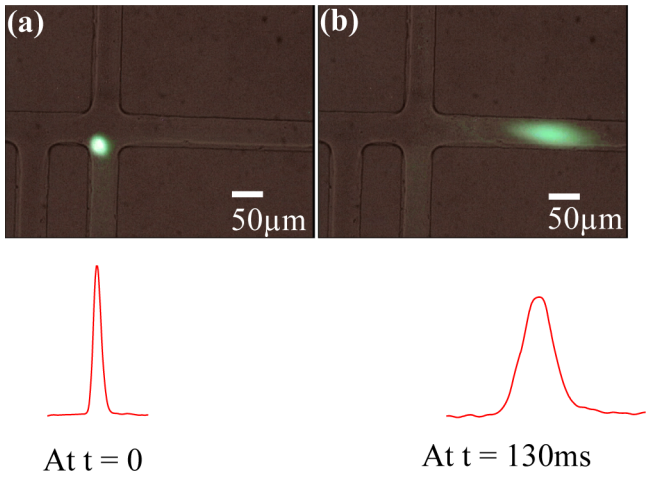

Figure 2. 20× magnified images of intact cell prior to lysis and the cell lysate. At t = 0, cell is at ZDP and produces a tall narrow peak. After 130 ms, a broader peak (4σ = ∼160 μm) is produced by the lysate moving along the separation channel under the influence of a 750 V/cm electric field.

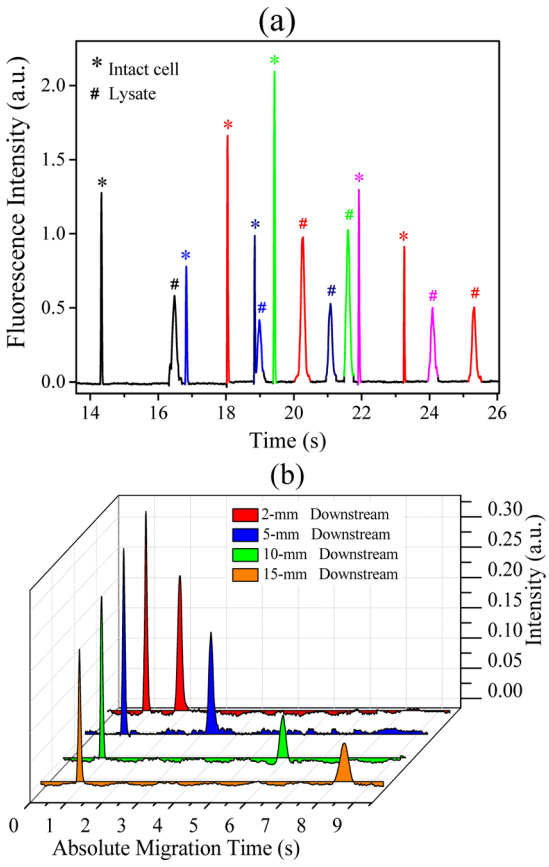

Figure 3. (a) Electropherogram of single cells using the optical fiber bridge. The detection point is 5 mm downstream of the lysis intersection. Each cell produces two peaks. The first narrow peak corresponds to the ZDP. The second broader peak that appears ∼2 s after the first peak is obtained at the LDP. (b) Single cell electropherograms obtained with the optical fiber bridge as a function of separation distance.

the same within experimental error indicating a symmetric distribution of values and little migration time drift. This trend can be seen for all four separation distances (Table S1). The

Table 1. Variation of Absolute Migration Time, RSD % of Absolute Migration Time, Drift in Absolute Migration Time, and Injection Plug Velocities at 2 mm, 5 mm, 10 mm, and 15 mm Detection Distances

distance (mm)	avg absolute migration time (s)	RSD % of absolute migration time	drift of absolute migration time (%)	injection plug velocity (mm/s)	no. of cells
2	0.99 ± 0.08	8.4	4.8	2.04 ± 0.18	83
5	2.40 ± 0.10	4.1	6.0	2.08 ± 0.085	111
10	5.14 ± 0.06	1.2	1.3	1.94 ± 0.022	74
15	7.25 ± 0.08	1.1	0.3	2.07 ± 0.023	75

absolute precision values for all of the migration distances were small and similar indicating good robustness for the technique. The small analyte migration time variation at each distance was probably due to the lateral location of the cell in the lysis intersection when lysed and small fluctuations in the hydrodynamic flow. These absolute values also agree with the previous work performed in our lab using relative migration times instead of absolute migration times.[16] The % RSD decreased significantly as separation distance increased as seen in Table 1 and Figures S2 and S4. Similar trends were observed for migration time drift (Table 1). The separation velocities at all separation distances were essentially constant as would be expected (Figure S3) The average velocity of the injection plug was 2.03 ± 0.06 mm/s over all distances. For all runs, the prelysis/separation peak area ratios were nearly constant indicating that the injection efficiency was constant over the course of any particular run. The ratio was not 1:1 due to excitation and emission-coupling inefficiencies with the fiber and migration velocity differences between the intact cell and the lysate as discussed above.

Under ideal circumstances, lysate peaks will be broadened as a function of separation distance solely due to longitudinal (molecular or Fickian) diffusion. Longitudinal diffusion can be determined using the Einstein−Smoluchowski equation ($\sigma^2 = 2Dt$) where σ^2 is the spatial peak variance, D is the diffusion coefficient, and t is the migration time. The diffusion coefficient (D) is 1/2 the slope of the plot of spatial peak variance vs migration time. The y-intercept is the variance due to the injection plug length and detection window length.[22,23] The slope of a plot of the spatial peak variance (σ^2) versus migration time (t) (Figure S5) for the data reported above yielded an experimentally derived diffusion coefficient for CFDA of 4.93 × 10^{-5} cm^2 s^{-1} at 25 °C which is 11× greater than the static value for fluorescein previously reported (4.25 × 10^{-6} cm^2 s^{-1} at 23 °C).[22] The excess dispersion, i.e., band broadening in excess of molecular diffusion, is likely due to Joule heating, the cell-separation buffer conductivity mismatch, and/or hydrodynamic flow generated by the on-chip, in-channel pumps. The injection plug length (l) was determined from the y-intercept ($l_{inj}^2/12$) of the graph minus the detection window length ($l_{det}^2/12$).[23] The detection window length was determined by the (pinhole aperture)/(objective magnification) which was equal to 40 μm. The calculated average l_{inj} value (at t = 0) over all four runs was 65 μm and consistent with that seen experimentally. (In Figure 2, the lysate bandwidth at 4σ after 130 ms is ∼160 μm.) Finally, the ability to calculate the absolute migration time and to measure peak width also allows the calculation of the separation efficiency (number of theoretical plates generated, N). A plot of N vs the separation distance (Figure S6) yielded a straight line as expected (R^2 = 0.96, see the Supporting Information) with

DOI: 10.1021/acs.analchem.6b03133
Anal. Chem. 2016, 88, 9920−9925

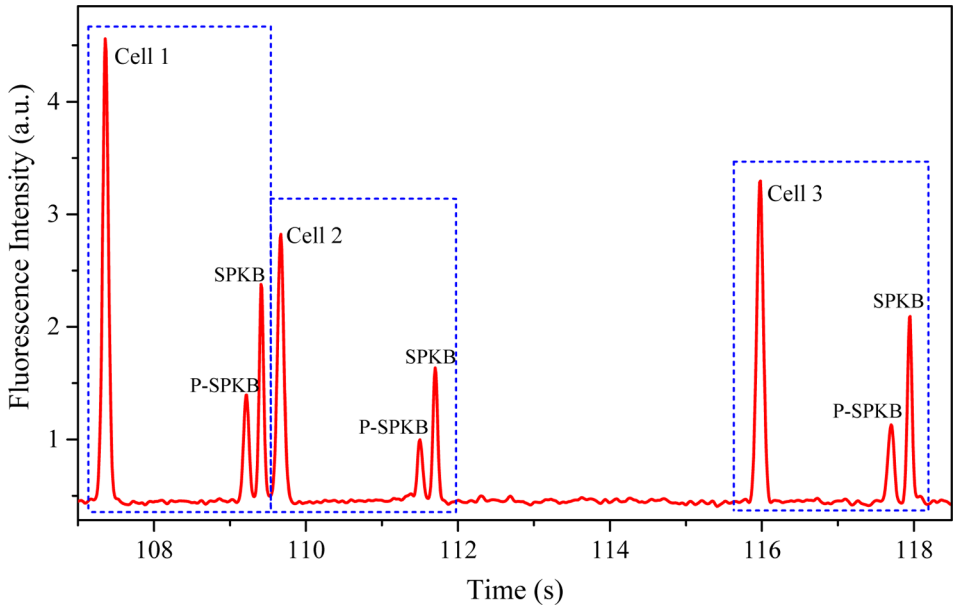

Figure 4. Electropherogram of PKB and p-PKB substrates (SPKB and P-SPKB, respectively) released from single T-lymphocytes. Intact cells were detected by fiber at ZDP. PKB and p-PKB substrates were detected 2 mm downstream of the lysis intersection in the separation channel.

an average plate height (H) of 4.3 μm for the single cell separations.

Detection of PKB Phosphorylated and Nonphosphorylated Substrates from Single Cells. PKB (also known as Akt; serine/threonine kinase) plays key roles in many vital cellular functions (i.e., glucose metabolism,[24] insulin production,[25] and apoptosis[26]). Biomedical and pharmaceutical industries have broad interests in better understanding kinase pathways as misregulation of these pathways leads to a variety of diseases.[27,28] Previous work from the Allbritton group has shown that kinase activity in single cells can be monitored through the addition of a peptide substrate that contains the amino acid sequence specific for that kinase.[17,29,30] Chemical moieties that can be attached to the peptide have also been identified in order to passively transport the peptide across a cell membrane.[20,31] In the experiment reported below, a myristoyl group was attached to a fluorescently labeled decapeptide specific for PKB. In addition, a cysteine and disulfide linkage between the substrate peptide and the peptide containing the myristoyl group was included. The myristoyl group is known to be a carrier molecule for peptide cargos in cell loading as shown by the Albritton group. It inserts the cargo to which it is attached, through the cell membrane via "flip-flop diffusion".[20] Once the cargo has diffused into the cell, peptide substrate is released from the carrier molecule due the reducing environment in cytoplasm. If PKB is active it will phosphorylate the threonine in the peptide. The activity of PKB can then be monitored by examining the ratio of the phosphorylated and nonphosphorylated peptides electrophoretically separated in the cell lysate as reported previously.[30] For inactive or highly active kinases, only the nonphosphorylated or phosphorylated peptides, respectively, may be present. Under such conditions, the ability to measure absolute migration times of the analyte(s) is critical to identify what specie(s) are in the cell. The implementation of an optical fiber bridge in the microfluidic device allows the measurement of the absolute migration time and thus such identification to be made. Figure 4 demonstrates the separation of phosphorylated and nonphosphorylated PKB from Jurkat cell lysate. A total of 25 cells were separated over the course of 310 s for an analysis rate of ~5 cells/min. The absolute migration times of phosphorylated and nonphosphorylated substrates were 1.80 ± 0.06 s and 2.03 ± 0.05 s, respectively. This initial result will, however, need to be confirmed with additional experiments. In the future, results from the addition of multiple kinases and the effects of the addition of agonists/antagonists/inhibitors/stimulators of kinases will be reported using this microfluidic setup at the single cell level.

CONCLUSIONS

The two-layer microfluidic device reported above allowed the detection of hundreds of single cells in short time period (<15 min). Two detection points were established at any two points of interest using an out-of-plane multimode optical fiber bridge that transmitted both excitation and emission light two ways. The detection distances were easily changed without modifying the microfluidic manifold. The two points of interests were excited simultaneously with a single excitation (488 nm) source and detected with a single photomultiplier tube. With this design the absolute migration times for cell lysates were measured. This allowed the determination of migration time drift, lysate injection efficiency, band broadening, and separation efficiency, parameters that could not be determined easily previously. In addition to providing the ability to better monitor and evaluate separation characteristics, this setup could be applied to a variety of other analytical applications including monitoring the velocity of particles, cells, or droplets in microfluidic systems. As an example of such an application, the separation of phosphorylated and nonphosphorylated kinase substrate peptides from single cell lysates was reported.

ASSOCIATED CONTENT

Supporting Information

The Supporting Information is available free of charge on the ACS Publications website at DOI: 10.1021/acs.analchem.6b03133.

DOI: 10.1021/acs.analchem.6b03133
Anal. Chem. 2016, 88, 9920−9925

Detailed list of chemicals and reagents; description of the fluorescent peptide synthesis; sample preparation and microchip operation details; theoretical and experimental investigations of the transmission and coupling efficiency of the bridged fiber configuration; additional data on cell lysis times, migration time distribution, diffusion and injection plug analysis; and figures of absolute migration time, average velocity, peak variance, and separation efficiency as a function of separation distance (PDF)

AUTHOR INFORMATION

Corresponding Author

*E-mail: culbert@ksu.edu. Phone: 785-532-6685. Fax: 785-532-6666.

Author Contributions

§D.E.W.P. and J.S. contributed equally to the paper.

Notes

The authors declare no competing financial interest.

ACKNOWLEDGMENTS

This research was funded by NSF Grants CHE-1411993 and CBET-1159966. D.E.W.P. was supported by the Johnson Cancer Center, Kansas State University.

REFERENCES

(1) Godin, J.; Chen, C.-H.; Cho, S. H.; Qiao, W.; Tsai, F.; Lo, Y.-H. *J. Biophotonics* **2008**, *1*, 355−376.

(2) Patabadige, D. E.; Jia, S.; Sibbitts, J.; Sadeghi, J.; Sellens, K.; Culbertson, C. T. *Anal. Chem.* **2016**, *88*, 320−338.

(3) Tang, S. K. Y.; Stan, C. A.; Whitesides, G. M. *Lab Chip* **2008**, *8*, 395−401.

(4) Baylor, M.-E.; Cerjan, B. W.; Pfiefer, C. R.; Boyne, R. W.; Couch, C. L.; Cramer, N. B.; Bowman, C. N.; McLeod, R. R. *Opt. Mater. Express* **2012**, *2*, 1548−1555.

(5) Spicer, D.; McMullin, J. N.; Rourke, H. *J. Micromech. Microeng.* **2006**, *16*, 1674−1680.

(6) Mogensen, K. B.; Petersen, N. J.; Hubner, J.; Kutter, J. P. *Electrophoresis* **2001**, *22*, 3930−3938.

(7) McMullin, J. N.; Qiao, H.; Goel, S.; Ren, C. L.; Li, D. *J. Micromech. Microeng.* **2005**, *15*, 1810−1816.

(8) Pires, N. M.; Dong, T.; Hanke, U.; Hoivik, N. *Sensors* **2014**, *14*, 15458−15479.

(9) Guo, F.; Lapsley, M. I.; Nawaz, A. A.; Zhao, Y.; Lin, S. C.; Chen, Y.; Yang, S.; Zhao, X. Z.; Huang, T. J. *Anal. Chem.* **2012**, *84*, 10745−10749.

(10) Remmerbach, T. W.; Wottawah, F.; Dietrich, J.; Lincoln, B.; Wittekind, C.; Guck, J. *Cancer Res.* **2009**, *69*, 1728−1732.

(11) Faigle, C.; Lautenschlager, F.; Whyte, G.; Homewood, P.; Martin-Badosa, E.; Guck, J. *Lab Chip* **2015**, *15*, 1267−1275.

(12) Imai, K.; Okazaki, T.; Hata, N.; Taguchi, S.; Sugawara, K.; Kuramitz, H. *Anal. Chem.* **2015**, *87*, 2375−2382.

(13) Kovarik, M. L.; Shah, P. K.; Armistead, P. M.; Allbritton, N. L. *Anal. Chem. (Washington, DC, U. S.)* **2013**, *85*, 4991−4997.

(14) Kovarik, M. L.; Dickinson, A. J.; Roy, P.; Poonnen, R. A.; Fine, J. P.; Allbritton, N. L. *Integr. Biol.* **2014**, *6*, 164−174.

(15) Phillips, K. S.; Lai, H. H.; Johnson, E.; Sims, C. E.; Allbritton, N. L. *Lab Chip* **2011**, *11*, 1333−1341.

(16) McClain, M. A.; Culbertson, C. T.; Jacobson, S. C.; Allbritton, N. L.; Sims, C. E.; Ramsey, J. M. *Anal. Chem.* **2003**, *75*, 5646−5655.

(17) Proctor, A.; Herrera-Loeza, S. G.; Wang, Q.; Lawrence, D. S.; Yeh, J. J.; Allbritton, N. L. *Anal. Chem.* **2014**, *86*, 4573−4580.

(18) Patabadige, D. E. W.; Mickleburgh, T.; Ferris, L.; Brummer, G.; Culbertson, A. H.; Culbertson, C. T. *Electrophoresis* **2016**, *37*, 1337−1344.

(19) Wang, H.; Udukala, D. N.; Samarakoon, T. N.; Basel, M. T.; Kalita, M.; Abayaweera, G.; Manawadu, H.; Malalasekera, A.; Robinson, C.; Villanueva, D.; Maynez, P.; Bossmann, L.; Riedy, E.; Barriga, J.; Wang, N.; Li, P.; Higgins, D. A.; Zhu, G.; Troyer, D. L.; Bossmann, S. H. *Photochem. Photobiol. Sci.* **2014**, *13*, 231−240.

(20) Nelson, A. R.; Borland, L.; Allbritton, N. L.; Sims, C. E. *Biochemistry* **2007**, *46*, 14771−14781.

(21) Poulsen, C. R.; Culbertson, C. T.; Jacobson, S. C.; Ramsey, J. M. *Anal. Chem.* **2005**, *77*, 667−672.

(22) Culbertson, C. T.; Jacobson, S. C.; Ramsey, J. M. *Talanta* **2002**, *56*, 365−373.

(23) Jacobson, S. C.; Culbertson, C. T. In *Separation Methods in Microanalytical Systems*; Kutter, J. P., Fintschenko, Y., Eds.; CRC Press LLC: Boca Raton, FL, 2006; pp 19−54.

(24) Buzzi, F.; Xu, L.; Zuellig, R. A.; Boller, S. B.; Spinas, G. A.; Hynx, D.; Chang, Z.; Yang, Z.; Hemmings, B. A.; Tschopp, O. *Molecular and cellular biology* **2010**, *30*, 601−612.

(25) Welsh, G.; Hers, I.; Berwick, D.; Dell, G.; Wherlock, M.; Birkin, R.; Leney, S.; Tavare, J. *Biochem. Soc. Trans.* **2005**, *33*, 346−349.

(26) Duronio, V. *Biochem. J.* **2008**, *415*, 333−344.

(27) Scheid, M. P.; Woodgett, J. R. *Nat. Rev. Mol. Cell Biol.* **2001**, *2*, 760−768.

(28) Song, G.; Ouyang, G.; Bao, S. *J. Cell. Mol. Med.* **2005**, *9*, 59−71.

(29) Dickinson, A. J.; Hunsucker, S. A.; Armistead, P. M.; Allbritton, N. L. *Anal. Bioanal. Chem.* **2014**, *406*, 7027−7036.

(30) Meredith, G. D.; Sims, C. E.; Soughayer, J. S.; Allbritton, N. L. *Nat. Biotechnol.* **2000**, *18*, 309−312.

(31) Bechara, C.; Sagan, S. *FEBS Lett.* **2013**, *587*, 1693−1702.

DOI: 10.1021/acs.analchem.6b03133
Anal. Chem. 2016, 88, 9920−9925